

1 **Supporting information**

2 **Using oscillation to improve the insertion depth and consistency of hollow**
3 **microneedles for transdermal insulin delivery with mechanistic insights**

4

5 Fiona Smith ^a, Anna M. Kotowska ^a, Benjamin Fiedler ^{a†}, Edward Cerny ^b, Karmen
6 Cheung ^b, Catrin S. Rutland ^c, Faz Chowdhury^b, Joel Segal^d, Frankie J. Rawson^a & Maria
7 Marlow^{a*}

8

9 ^a School of Pharmacy, University of Nottingham, Nottingham NG7 2RD, United Kingdom

10 ^b Nemauro Pharma Limited, Advanced Technology Centre, Oakwood Drive,
11 Loughborough, Leicestershire LE11 3QF, United Kingdom

12 ^c School of Veterinary Medicine and Science, The University of Nottingham, NG7 2RD,
13 UK

14 ^d Department of Mechanical, Materials and Manufacturing Engineering, Faculty of
15 Engineering, University of Nottingham, Nottingham NG8 1BB, United Kingdom

16 [†] School of Pharmacy, University College London, London, WC1N 1AX, United Kingdom

17

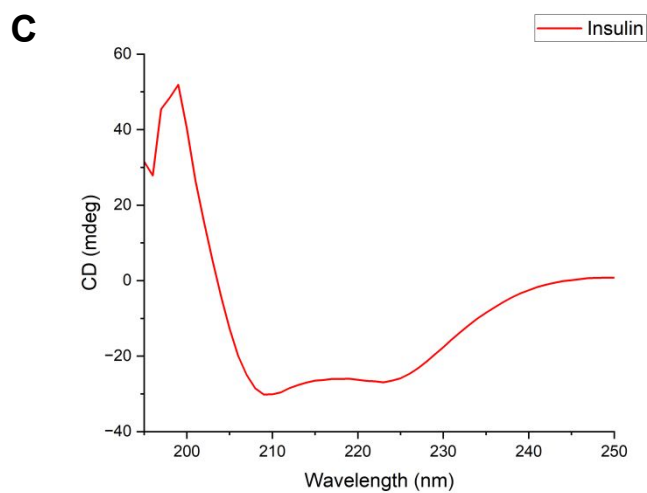
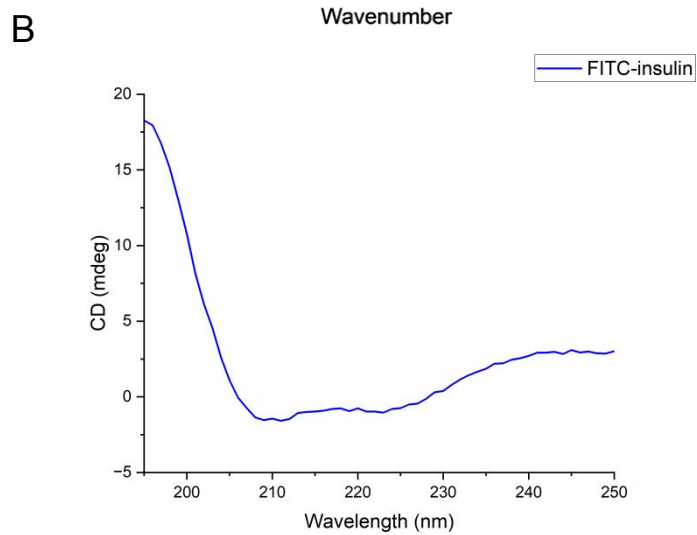
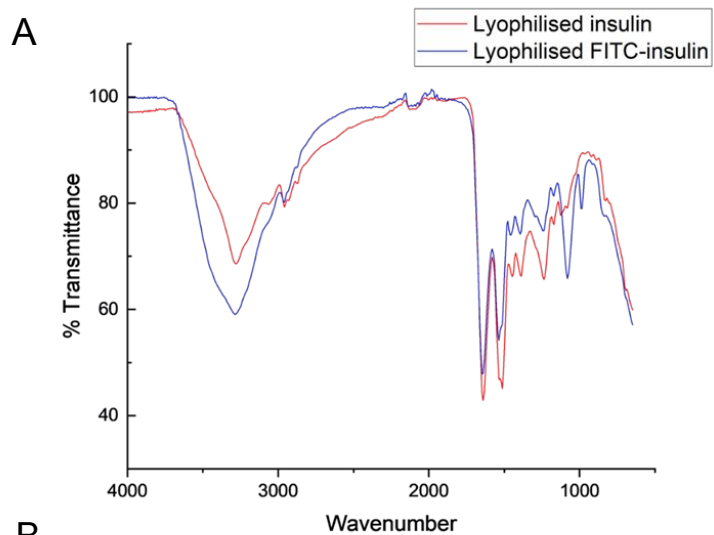
18 *Corresponding author: Maria.Marlow@nottingham.ac.uk, Tel.: 0115 8467045

19

20

21 Circular dichroism (CD)

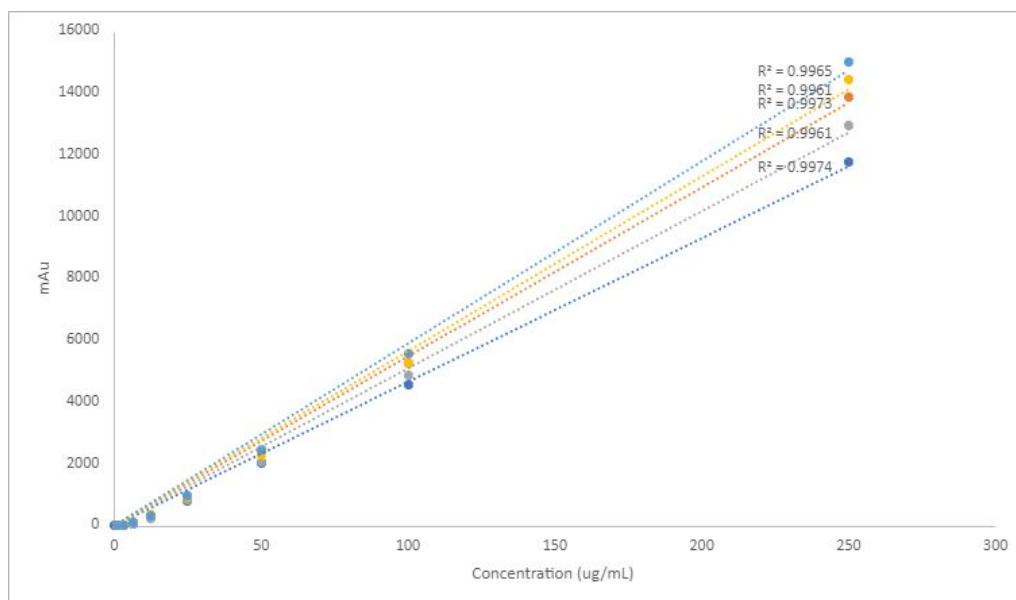
22 Before use, the CD (Chirascan VX, Applied Photophysics Limited, UK) was purged with
23 nitrogen gas to deplete oxygen in the system. Reconstituted insulin (both naked and
24 tagged) was diluted 1:200 with HPLC grade water and loaded into a 1 mm high precision
25 quartz cuvette (Hellma Analytics). The temperature was monitored throughout each run
26 and stayed constant between 21.7-21.9 °C. Spectra were recorded between 190 and 280
27 nm. Step size was 1 nm, bandwidth was 1 nm, count rate was 20,000 and acquisition
28 time was 0.5 seconds. Three repeat scans were completed for each sample, the average
29 calculated and plotted using OriginLab (Pro) 2023. Between runs, the cell was thoroughly
30 washed and dried to avoid contamination and stored in Hellmanex solution after use.



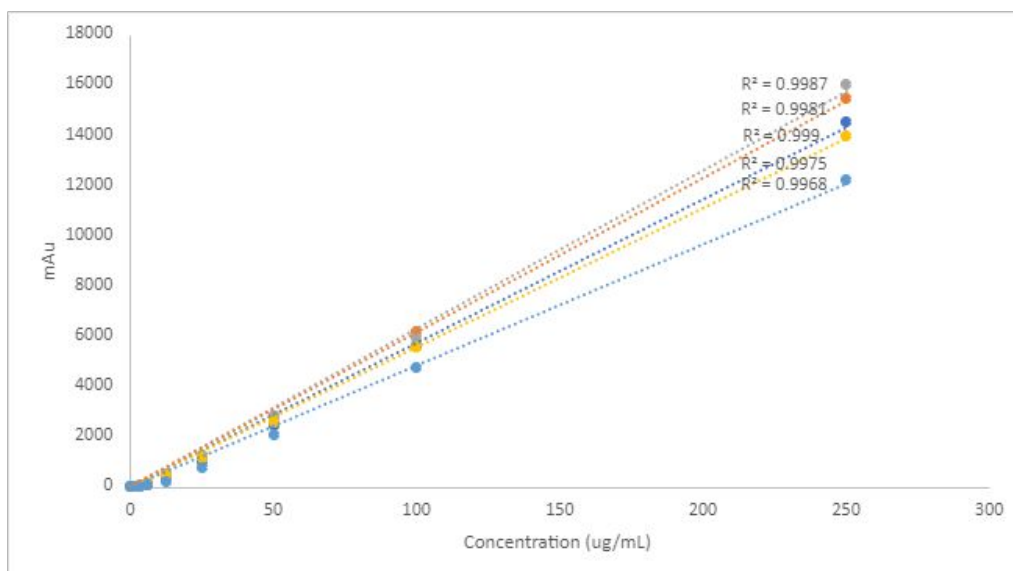
32 **Figure SI1:** Analysis of synthesised FITC-insulin showing A) the FT-IR spectra of
33 lyophilised insulin with FITC-insulin overlaid. Amide peaks are identifiable between
34 $1500-1600\text{ cm}^{-1}$ and $1600-1700\text{ cm}^{-1}$, whilst a peak representing the isothiocyanate
35 groups is present in the FITC-insulin sample at 1080 cm^{-1} and B) CD spectra with peaks
36 identifiable at 208 nm and 222 nm , demonstrating the method used for the synthesis of
37 the FITC-insulin does not detrimentally alter the native insulin structure, shown in C).
38 These analyses confirm the successful conjugation between FITC and insulin without
39 disrupting the insulin secondary structure.

40 HPLC method development

41 Standard curves with concentrations of 0, 1, 3.125, 6.25, 12.5, 25, 50, 100 and 250 $\mu\text{g/mL}$
42 of insulin, diluted in PBS, were prepared. To assess intra-variability, five standard curves
43 were run on the same day (Figure SI2). Separately, five standard curves of the same
44 concentrations, were run on different days to assess inter-variability (Figure SI3).



45
46 **Figure SI2:** Standard curves for 0, 1, 3.125, 6.25, 12.5, 25, 50, 100 and 250 $\mu\text{g/mL}$
47 concentrations of recombinant human insulin diluted in PBS using HPLC detection,
48 completed five times during the same HPLC run, used to determine intra-variability.



49

50 **Figure S13:** Standard curves for 0, 1, 3.125, 6.25, 12.5, 25, 50, 100 and 250 µg/mL
 51 concentrations of recombinant human insulin diluted in PBS using HPLC detection,
 52 completed on five separate occasions, used to determine inter-variability.

53 Using the signal-to-noise ratio, the limit of detection (LOD) and limit of quantification
 54 (LOQ) were determined. The LOD was determined as 1 µg/mL as the ratio frequently
 55 exceeded 3:1. An insulin concentration of 6.25 µg/mL reliably produced a STN ratio of
 56 over 10:1, whilst the lower concentration of 3.125 µg/mL did not. As such, 6.25 µg/mL
 57 was determined to be the LOQ, however it is likely that the true LOQ is lower than this.

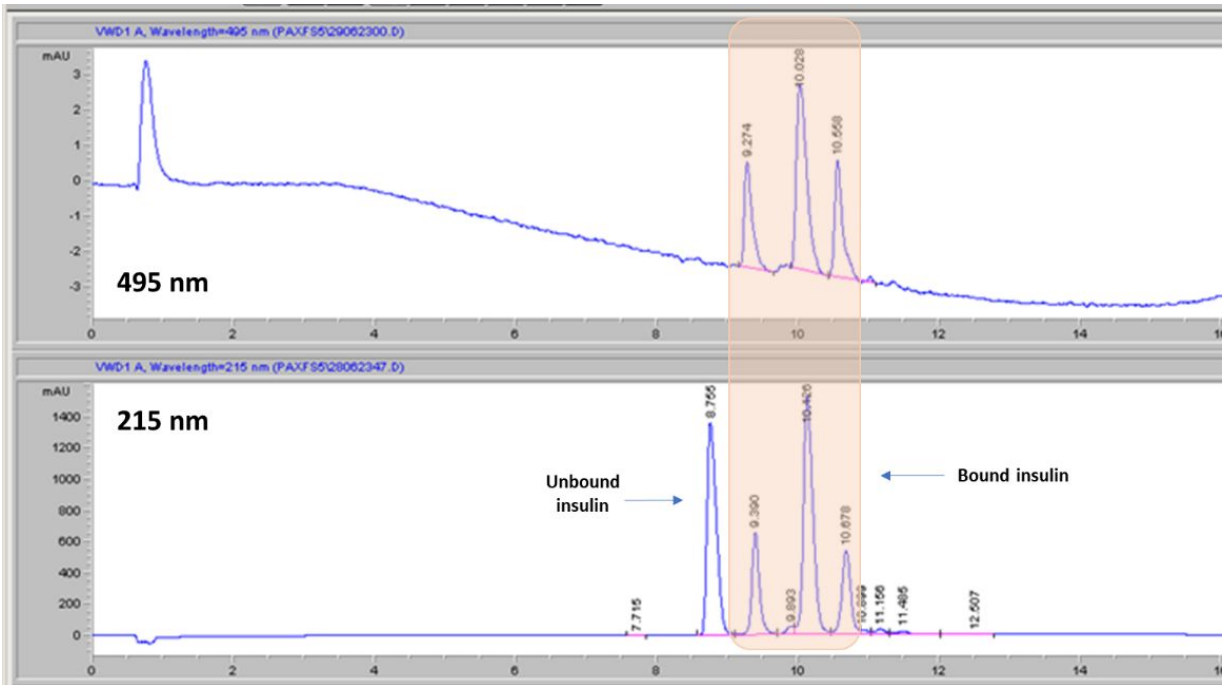
58 HPLC of FITC-insulin

59 In terms of FITC conjugation, the reactivity of amines at different chain positions in insulin
 60 differs. The phenylalanine at position B1 is the most reactive, followed by the glycine at
 61 A1, then the lysine at B29. As such, referring to early work by Jacob et al. and Hentz et
 62 al., it has been shown before that the elution pattern remains the same during HPLC
 63 analysis (1,2). Always first to elute is any unconjugated insulin. This is followed by FITC-
 64 insulin singularly conjugated at B1, then FITC-insulin singularly conjugated at A1, then
 65 FITC-insulin conjugated at both B1 and A1 locations and, finally, FITC-insulin tri-

66 conjugated at all three locations, B1, A1 and B29. This facilitates the identification of how
67 the FITC has conjugated with insulin for any FITC-insulin sample tested.

68 HPLC was employed to run a sample of the FITC-insulin at two different wavelengths,
69 215 nm and 495 nm respectively. 215 nm was used specifically to detect the insulin whilst
70 495 nm was to detect the FITC. Peaks were mapped according to the elution time.
71 Several peaks had the same elution time at the different wavelengths, which suggested
72 that the FITC reacted with the insulin at B1 (monosubstituted), A1 (monosubstituted) and
73 at both the B1 and A1 (disubstituted) sites. A single peak observed on the 215 nm spectra
74 suggested that a proportion of the insulin remained untagged by FITC. From the HPLC
75 data, it appears that most of the unconjugated FITC had been successfully removed
76 during the purification steps as a peak attributable to the FITC alone was not identified.
77 Small peaks observed between the major peaks have been observed previously and are
78 likely attributable to impurities in the FITC (1).

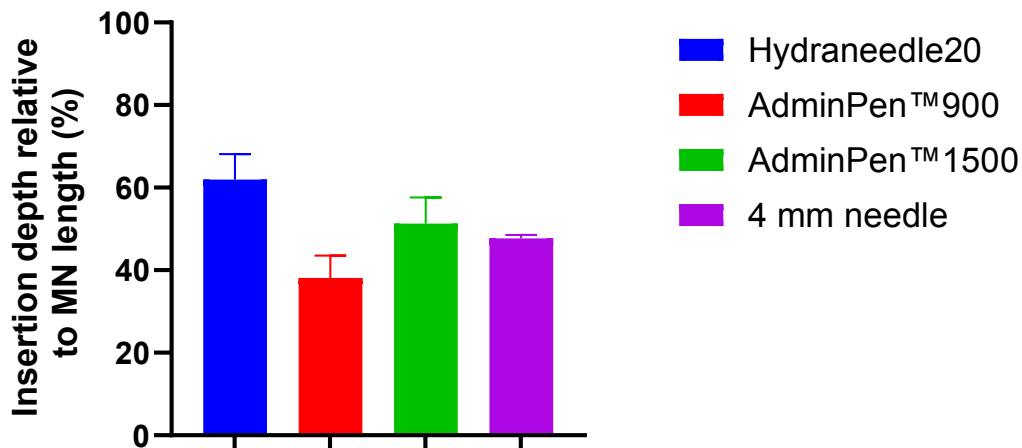
79 During the conjugation, a covalent thiourea bond is formed between the relevant amine
80 group of the insulin and the isothiocyanate group of the FITC. Thiourea bonds are known
81 to be stable. As such, it is unlikely that the thiourea bond would be broken upon injection
82 into the skin, giving providing confidence that FITC-insulin is a valuable tool for
83 understanding insulin distribution post administration.



84

85 **Figure S14:** HPLC chromatogram of FITC-insulin with UV detection at 215 nm (used to
 86 detect insulin) and 495 nm (used to detect FITC) demonstrating that the FITC has 3
 87 different conjugates. Some insulin remains unbound to FITC as shown by the peak at
 88 8.8 minutes.

89 Ex vivo insertion with commercially available hollow MNs



90

91 **Figure S15:** An ex vivo study comparing the depth of insertion into porcine skin
 92 achieved relative to the length of the MN/needle inserted. The Hydranneedle20 (500 μ m),
 93 AdminPen™ 900 (800 μ m), AdminPen™ 1500 (1400 μ m) and a 4 mm 31-gauge
 94 hypodermic needle were compared. The recorded insertion depth is considerably less

95 *than the MN length in each case, demonstrating incomplete needle insertion into the*
96 *skin. Data expressed as mean \pm SEM, n=3.*

97 Full factorial design of experiments

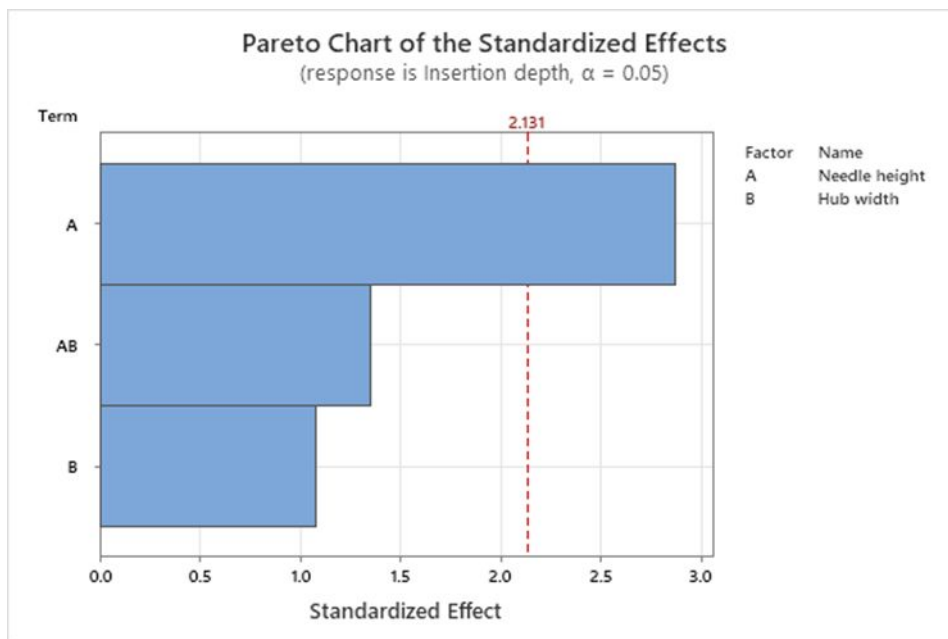
98 MiniTab 21 Statistical Software was selected to design a full-factorial design of
99 experiments (DOE). The aim was to understand whether there was a relationship
100 between needle length and the hub diameter and how this affects the insertion profile.
101 Five single hollow MNs, with dimensions listed in Table S11, were produced based upon
102 the upper and lower limits of parameters input into the software (needle height: lower limit
103 200 μ m and upper limit 1000 μ m, hub width: lower limit 2 mm, upper limit 10 mm), as
104 described in Section 2.3. Each MN was inserted into *ex vivo* porcine skin 4 times and
105 channel depth was measured using the methodology described in Section 2.5. A random
106 run-order was dictated by the software to reduce bias, listed in Table S13.

107 **Table S11:** DOE run order generated in a random sequence by MiniTab 21 Statistical
108 Software to reduce bias.

Run order	Needle length (μ m)	Hub width (mm)
1	200	10
2	1000	10
3	600	6
4	1000	2
5	600	6
6	200	2
7	1000	2
8	600	6
9	1000	2
10	200	2
11	1000	2
12	600	6

13	1000	10
14	1000	10
15	1000	10
16	200	2
17	200	10
18	200	2
19	200	10
20	200	10

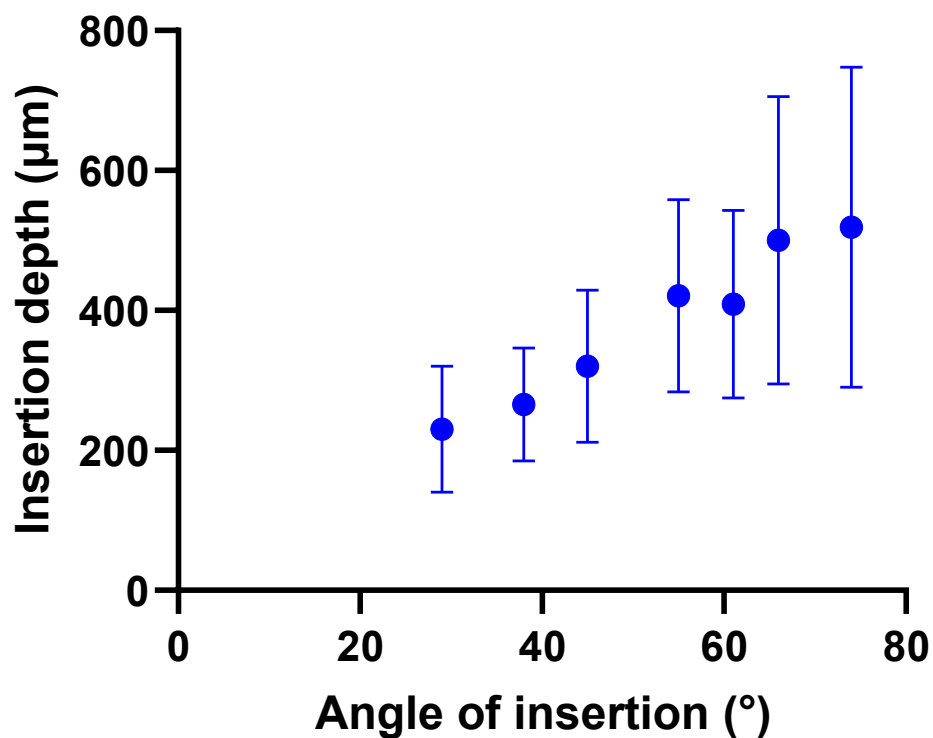
109



110 **Figure S16:** Pareto chart of the standardised effects visualising whether hub width,
 111 needle height or the relationship between the two have a statistically significant effect
 112 on achievable insertion depth by crossing the red dashed line if so. Needle height was
 113 determined to have a statistically significant effect ($p=0.012$) whilst hub width and the
 114 interaction between hub width and needle height were not.

115 The effect of angle on insertion depth

116 A mount was developed incorporating cork-covered wood, with the capability to vary the
 117 angle it rests. *Ex vivo* porcine skin was positioned on top of the cork before completing
 118 an insertion study (Section 2.5), allowing exploration of the effect of the angle of insertion
 119 on the insertion depth of a 1000 μm single hollow MN.



120

121 **Figure S17:** Insertion of a single hollow MN into ex vivo porcine skin when the angle of
 122 insertion is varied. The relationship shows that insertion depth increased in relation to
 123 the angle. The considerable standard deviation of insertion depth achieved highlights
 124 that consistency of insertion depth remains an issue even as penetration depth
 125 increases ($n=5 \pm SD$).

126

127 References

- 128 1. Hentz NG, Richardson JM, Sportsman JR, Daijo J, Sittampalam GS. Synthesis
 129 and Characterization of Insulin-Fluorescein Derivatives for Bioanalytical
 130 Applications. Anal Chem [Internet]. 1997;69(24):4994–5000. Available from:
 131 <https://pubs.acs.org/sharingguidelines>

132

133 2. Jacob D, Joan Taylor M, Tomlins P, Sahota TS. Synthesis and Identification of
134 FITC-Insulin Conjugates Produced Using Human Insulin and Insulin Analogues
135 for Biomedical Applications. J Fluoresc. 2016 Mar 1;26(2):617–29.

136